A pH-sensitive Xylan-based Superabsorbent Hydrogel for the Removal of Methylene Blue from Water

Yan Lin,[a,b,*] Guigan Fang,[a,b,*] Yongjun Deng,[a,b] Kuizhong Shen,[a,b] Chen Huang,[a,b] and Ting Wu [a,b]

A novel porous xylan-based hydrogel was prepared using methacrylated xylan and acrylic acid *via* free radical polymerization. The structure, morphology, and thermal stability of the hydrogel were characterized using Fourier transform infrared spectroscopy (FT-IR), scanning electron microscopy (SEM), and thermogravimetric analysis (TGA). The pH value had an important effect on the swelling and dye-adsorption properties of the hydrogel. When methylene blue was used as a dye model, the dye adsorption of the hydrogel followed the Langmuir isotherm model and pseudo-second order kinetic model. The calculated maximum adsorption capacity reached 4720 mg/g. Besides, the hydrogel retained about 90% of its adsorptive capacity even after 4 cycles of usage. Therefore, the xylan-based hydrogel presented excellent dye adsorption performance and could be a promising superabsorbent for wastewater treatment.

Keywords: Xylan; Superabsorbent; pH-sensitive; Adsorption; Methylene blue

*Contact information: a: Institute of Chemical Industry of Forestry Products, CAF; Key Lab of Biomass Energy and Material, Jiangsu Province; Key and Open Lab on Forest Chemical Engineering, SFA; National Engineering Lab for Biomass Chemical Utilization; Nanjing 210042, PR China; b: Collaborative Innovation Center for High Efficient Processing and Utilization of Forestry Resources, Nanjing Forestry University, Nanjing 210037, PR China; *Corresponding authors: linyan@icifp.cn; fangguigan@icifp.cn*

INTRODUCTION

With rapid economic growth and increased industrialization, water contamination by organic dyes has become a serious environmental issue and has caused widespread concern (Kumari *et al.* 2016). Colored industrial effluents can be highly toxic and carcinogenic, thus causing a great danger to living organisms. Because of the complex chemical structure, high hydrophilicity, and stability, the organic dye effluents pose difficulties for wastewater treatment (Mohammed *et al.* 2015). Many technologies have been used to treat colored wastewater, including coagulation and flocculation, oxidation, adsorption, membrane separation, and electro-coagulation methods (Wang *et al.* 2013; Katheresan *et al.* 2018; Li *et al.* 2019). Among these, the adsorption method is regarded as one of the most attractive processes because of its easy operation and high removal efficiency (Tang *et al*. 2013). It is crucial to develop high performance adsorbents for removing the pollutants. Recently, special attention has been paid to adsorbents based on natural polymers, such as cellulose, chitosan, and starch (Gomes *et al.* 2015; de Azevedo *et al.* 2017; Dai *et al.* 2018; Melo *et al*. 2018). Meanwhile, natural polymers contain abundant functional groups, which are of importance for the removal of organic dyes (Zhou *et al.* 2011; Yu *et al.* 2018).

Hemicellulose is one of the most abundant renewable polysaccharides found in nature. Hemicellulose-based adsorbents have been widely used to remove organic dyes from aqueous systems (Zhang *et al.* 2014; Song *et al.* 2016). Cheng *et al.* (2016) introduced

clay nanosheets into hemicellulose systems, forming hybrid hydrogels with admirable adsorption capacity for methylene blue (MB) at 148.8 mg/g. Sun *et al.* (2015a) prepared a stimuli-responsive hydrogel synthesized from wheat straw hemicelluloses using $CaCO_3$ as the porogen and used it for dye removal. Thus, novel hemicellulose-based hydrogels have attracted wide attention of researchers and showed great application potential as adsorbents for dye removal.

Xylan is the main type of hemicellulose in hardwood and is a part of the hemicelluloses of softwood and straw biomass. It exhibits the same properties as the other hemicelluloses, such as excellent hydrophilicity, biocompatibility, and biodegradability. So it is considered a promising raw material for developing novel adsorbents (Deng *et al.* 2014; Liu *et al.* 2018). Li and Buschle-Diller (2017) prepared a type of pectin-blended anionic xylan film for cationic-dyes adsorption. Jing (2014) introduced a novel superabsorbent based on multiwalled carbon nanotubes-xylan composite and poly-(methacrylic acid), and the maximum adsorption capacity was 192 mg/g. Qi *et al.* (2017) reported a xylan-modified graphene oxide for adsorption of organic dyes with the adsorption capacity nearly 700 mg/g. During recent decades, improvements in the performance of superabsorbents has played an important role in the field of functional polymers. However, few xylan-based hydrogels have been reported as superabsorbents for organic dyes adsorption.

This study investigated the preparation and evaluation of xylan-based hydrogels to adsorb MB from aqueous solutions. After modification, the xylan derivative was grafted with acrylic acid by free radical polymerization to prepare the superabsorbent. The xylan-based hydrogel thus prepared was characterized using Fourier transform infrared spectroscopy (FT-IR), scanning electron microscopy (SEM), and thermogravimetric analysis (TGA). The pH sensitivity of the hydrogel was evaluated in water and MB solutions. The kinetic behavior and isotherm analysis of MB adsorption on the hydrogel were investigated as well. Based on the results, the xylan-based hydrogel showed great adsorption performance of MB from aqueous solution.

EXPERIMENTAL

Materials

Pure xylan from beech wood, with the molecule weight of 38,500 g/mol, was purchased from SERVA Electrophoresis GmbH (Heidelberg, Germany). Glycidyl methacrylate (GMA) with the purity of 97% and containing 100 ppm hydroquinone methylether (MEHQ) as stabilizer, was purchased from Aladdin Industrial Inc. (Shanghai, China). Pure analytical grade MB was obtained from Tianjin Institute of Chemical Reagents (Tianjin, China). Other reagents used were of analytical grade and used without further purification. Ultrapure water with a resistivity of 18.25 MΩ·cm at 25 °C was used for all experiments.

Synthesis of Xylan-based Hydrogels

Xylan was modified with glycidyl methacrylate (GMA) using the reported procedure (Guilherme *et al.* 2005; Peng *et al.* 2012). About 3.3 g of xylan was dissolved in 100 mL of dimethyl sulfoxide (DMSO) at 95 °C. After the solution was cooled to room temperature, the catalyst 4-dimethylaminopyridine (DMAP, 0.66 g) was added, and the mixture was stirred at 40 °C for 0.5 h. Later, 2.0 g GMA was added and the final reaction

mixture was stirred for 24 h. After that, the reaction mixture was precipitated with 500 mL of anhydrous ethanol and filtered. The precipitate obtained was washed with anhydrous ethanol three times. Then the products were dissolved in water and freeze-dried at -50 °C for 72 h. The modified xylan thus obtained was light brown and was labeled as MX.

The modified xylan (MX, 0.083 g) was dissolved in 10 mL water and stirred at 60 °C in a water bath. Then ammonium persulfate (APS) solution, acrylic acid (AAc), and methylene-bis-acrylamide (MBA) were added sequentially. The reaction was continued for 4 h. After that, the hydrogels were taken out, washed with water, and cut into small pieces. Then the hydrogels were immersed in water for 72 h and the water was refreshed every 6 h. After vacuum drying at 40°C for 48 h, the xylan-based hydrogels were obtained as solid.

Characterization

The FT-IR spectra of xylan, modified xylan (MX), and the xylan-based hydrogel (MXH) were measured on a Nicolet iS10 model FT-IR spectrometer (Thermo Electron, Waltham, MA, USA) in the wavelength range from 4000 cm^{-1} to 500 cm^{-1}. The samples were freeze-dried at -50 °C for 72 h without other pretreatment before the FT-IR detection. The morphology of the xylan-based hydrogel was analyzed by SEM (Hitachi S-3400N, Tokyo, Japan). Prior analysis, the swollen hydrogel was freeze-dried at -50 °C for 72 h. Then it was fractured, and the interior surface was coated with gold by sputtering before SEM visualization. The TGA of the lyophilized hydrogel sample was performed using a TG209F1 Libra thermal analyzer (NETZSCH, Bavaria, Germany) in a nitrogen atmosphere with the gas flow of 20 mL/min. The temperature range used was from 40°C to 700 °C at a scan rate of 10 °C/min.

Swelling Experiments

The swelling property of the xylan-based hydrogel was measured using the previously reported method from the authors (Lin *et al.* 2018). The dried hydrogels were first immersed in water at 25 °C for 72 h. Then the swollen samples were taken out, wiped the water on the surface of samples, and then weighed. The weight of samples was measured three times to calculate the average result. The swelling ratio (S) of the hydrogel sample was calculated by Eq. 1,

$$S = (W\text{-}W_0)/W_0 \quad (1)$$

where W_0 (g) and W (g) denote the weights of dry and swollen hydrogel samples.

Adsorption Experiments

The adsorption performance of the xylan-based hydrogel as superabsorbent for MB removal was investigated in this study (Mall *et al.* 2005; Xu *et al.* 2018). The effects of pH value, initial MB concentration, and adsorption time on the dye adsorption were investigated. For evaluating the effect of pH value, the dried hydrogels (10 mg) were immersed in 30 mL MB solutions (100 mg/L) with different pH values and then placed in a 25 °C shaking incubator for 24 h with a constant rate of 100 rpm. The pH of the MB solutions was adjusted with 0.01 M HCl and 0.01 M NaOH solutions. The effect of initial MB concentration was studied at 50 mL MB solutions with various concentrations from 500 mg/L to 1800 mg/L and the pH was adjusted to 8. In order to study the adsorption kinetics, the experimental conditions were kept basically the same as that in pH investigation above, except that the MB solution (100 mg/L) was 50 mL and the pH was adjusted to 8. Then the hydrogel was separated at specific time intervals, and the

concentration of MB solutions was measured using an ultraviolet spectrophotometer (T6 New Century, Beijing, China) at 664 nm. The amount of MB (q) adsorbed was calculated using Eq. 2, and the removal ratio (R) was calculated by Eq. 3,

$$q = (C_0 - C_e) \times V/m \quad (2)$$

$$R = (C_0 - C_e)/C_0 \times 100\% \quad (3)$$

where C_0 (mg/L) and C_e (mg/L) are the initial and equilibrium concentrations of MB solution, respectively; V (L) is the volume of MB solution; and m (g) is the weight of the dry hydrogel.

Reuse Experiments

The reusability of xylan-based hydrogel for dye adsorption was studied by four cycles of adsorption-desorption processes. Approximately 10 mg dried xylan-based hdrogel was placed in 30 mL MB solution (100 mg/L, pH=8). After 2 h, the MB preloaded hydrogel was separated and immersed in 30 mL HCl (0.1 M) to restore the adsorption sites of the hydrogel. Later the restored hydrogel was washed with 30 mL water and used for the next adsorption-desorption cycle. The removal efficiency was calculated by the removal ratio of MB in order to investigate the reusability of the xylan-based superabsorbent.

RESULTS AND DISCUSSION

FT-IR Characterization

The FT-IR spectra of xylan, MX, and MXH are depicted in Fig.1. In Fig.1a, the intense band at 1032 cm^{-1} originated from the C-O-C stretching of pyranoid-ring on xylan. The absorbance at 3363 cm^{-1} resulted from the O-H stretching. Compared with Fig.1a, a characteristic peak at 1715 cm^{-1} found in Fig.1b was related to C=O stretching, which indicated that the methacrylate group was attached onto xylan molecule (Peng *et al.* 2012). Very wide absorbance at 3693 cm^{-1} to 2000 cm^{-1} in Fig. 1c was attributed to O-H stretching from -OH groups on xylan ring and grafted -COOH groups.

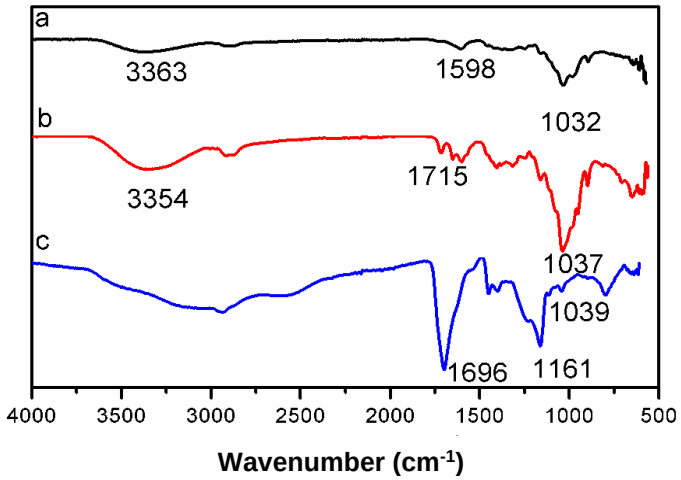

Fig. 1. FT-IR spectra of (a) xylan, (b) modified xylan, and (c) xylan-based hydrogel

The prominent absorbance at 1696 cm^{-1} was assigned to the overlap effects of the C=O stretching bands of carbonyl groups originated from the modified xylan, acrylic acid, and MBA (Guilherme *et al*. 2005; Paulino *et al.* 2006). The band at 1161 cm^{-1} was attributed to C-O and C-O-C bond stretchings (Peng *et al.* 2012).

Morphology Analysis

The interior morphology of the prepared MXH is shown in Fig. 2. The hydrogel exhibited a large number of pores and gaps with uneven size. This porous structure was convenient for the penetration of water and chemicals into the hydrogel network, resulting in the enhancement of water and dye adsorptions.

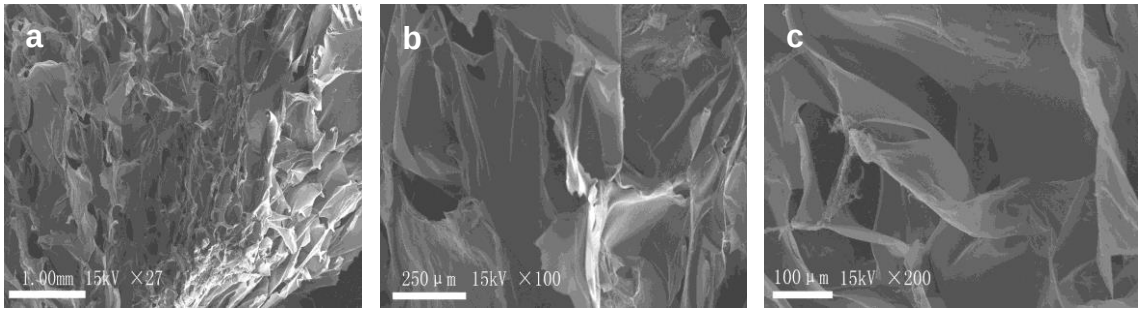

Fig. 2. SEM images of the xylan-based hydrogel sample (a: MXH×27; b: MXH×100; and c: MXH×200)

Thermogravimetric Analysis

The TGA and the corresponding differential thermogravimetric analysis (DTG) plots for xylan and MXH are shown in Figs. 3a and 3b, respectively. As can be seen in Fig. 3a, the xylan showed one distinct thermal degradation stage from 230 °C to 330 °C and the MXH showed two distinct thermal distinct degradation stages (200 °C to 280 °C, and 280 °C to 500 °C). It was reported that TGA of polyacrylic acid (PAAc) exhibited two distinct zones of weight loss, 100 °C to 250 °C and 250 °C to 500 °C (Chen *et al.* 2016). This indicates that PAAc chains were successfully grafted on the xylan backbone.

The DTG results (Fig. 3b) show a peak in xylan curve at about 252 °C due to xylan degradation. There were two peaks in the curve of xylan-based hydrogel at 252 °C and 415 °C because of the decomposition. Notably, the reported DTG peaks of PAAc were found at 260 °C and 430 °C, respectively (Chen *et al.* 2016). These results suggest that the thermal stability of the xylan-based hydrogel is unchanged when compared with xylan.

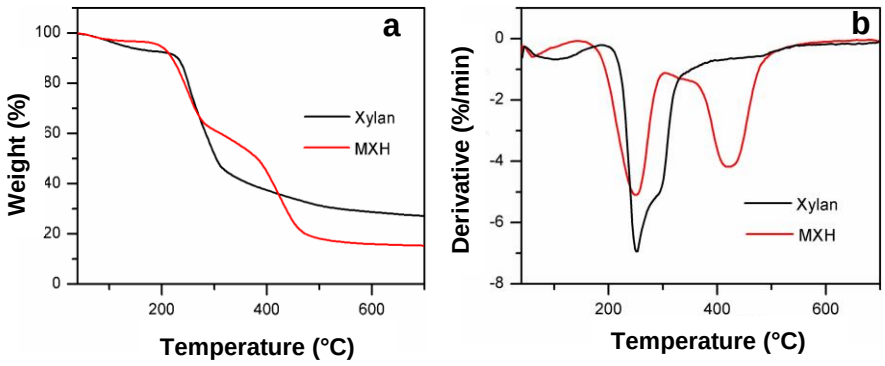

Fig. 3. TGA(a) and DTG (b) curves of xylan and xylan-based hydrogel (MXH-13)

Preparation and Swelling Property of the Xylan-based Hydrogels

In this work, the MXH superabsorbents were prepared by modified xylan and acrylic acid *via* free radical polymerization. The reaction between GMA and polysaccharides has been much studied in last decades (van Dijk-Wolthuis *et al.* 1995; van Dijk-Wolthuis *et al*. 1997; Paulino *et al.* 2010). It appeared that the reaction of xylan with GMA was a transesterification reaction rather than an opening epoxy ring of GMA, resulting in the direct attachment of methacryloyl group to xylan (Peng *et al.* 2012). The modification reaction of xylan was not the research emphasis for this study.

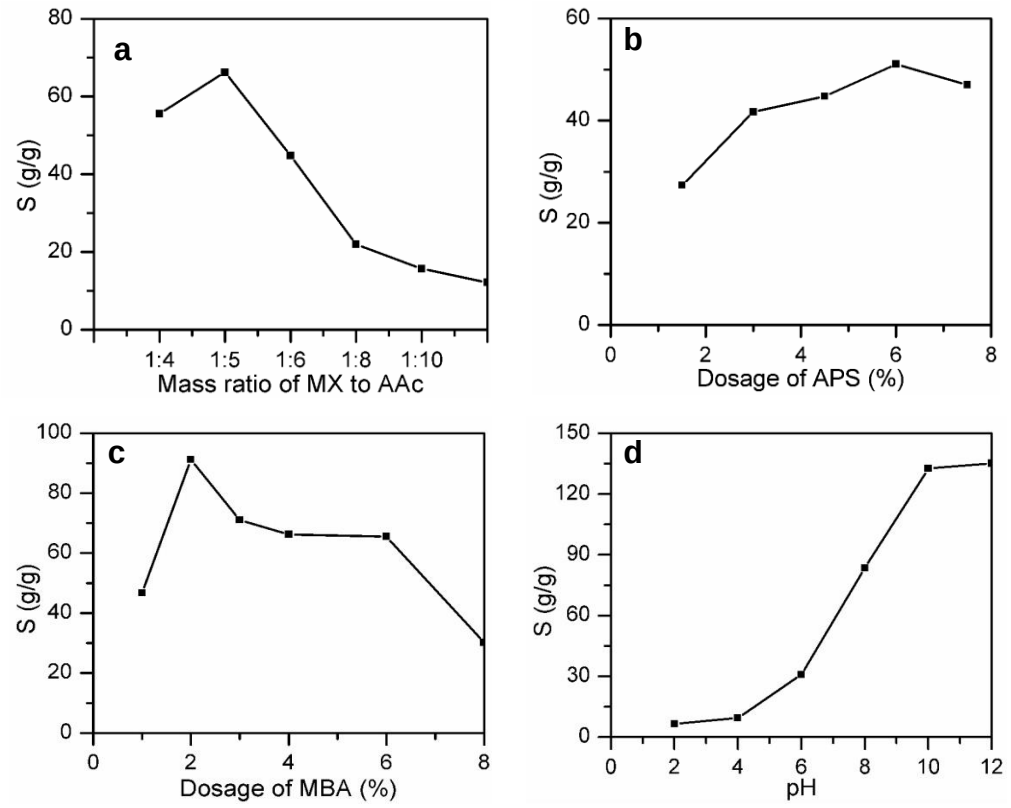

Fig. 4. Effects of mass ratios of MX to AAc (a), dosage of the APS (b), and dosage of MBA (c) on the swelling ratio of the hydrogels; swelling curve of MXH-13 (d). Reaction conditions: (a) APS dosage 6%, MBA dosage 2%, 60 °C, 4 h; (b) mass ratio1:6, APS dosage 6%, 60 °C, 4 h; (c) mass ratio1:5, APS dosage 6%, 60 °C, 4 h

Several MXH samples were prepared by varying (a) the mass ratio of MX to acrylic acid, (b) the dosage of APS, and (c) the dosage of MBA. The swelling ratio of the hydrogels was measured and is shown in Figs. 4a to 4c (the samples were labeled as MXH-1 to MXH-17, respectively). It can be seen that these three factors had noticeable effects on the water adsorption of the hydrogels. When the mass ratio of MX to AAc, dosage of APS, and dosage of MBA were increased, the swelling ratio of hydrogels increased to a maximum, and then they decreased in various degrees. Especially in Fig. 4a, if excess AAc was used in the reaction, the swelling ratio of the hydrogels was very low, which can be attributed to the self-polymerization of AAc. In Figs. 4b to 4c, excessive APS and MBA contents also played adverse effects on the swelling ratio of the hydrogels. When excess amounts of APS was added, self-polymerization of AAc was intensified and the chain termination reaction was aggravated, resulting in less carboxylic groups being linked onto the polymer

and resulting in decreased molecular weight of the hydrogel. Besides, more MBA content would intensify the crosslinking of hydrogels and give rise to tighter polymer network, thus reducing the swelling ratios. Therefore, the suitable preparation condition was as follows: 1:5 MX:AAc mass ratio, 6% (w/w) of APS dosage, and 2% (w/w) of MBA dosage. Under this condition, the maximum swelling ratio of the hydrogel (MXH-13) obtained was 91.2 g/g.

Figure 4d shows the swelling ratio of the hydrogel (MXH-13) at different pH values. It can be seen that the swelling ratio increased with increasing pH values from 2 to 10, and then reached a stable value. At a lower pH, COO^- groups in the hydrogel were protonated. The strong intramolecular and intermolecular hydrogen bonding between -COOH and -OH groups contributes to the shrinkage of the hydrogel network, which is bad for the water uptake. At higher pH, COO^- groups cause electrostatic repulsion forces among the adjacent ionized groups of hydrogel network. The swollen structure allows for large number of water uptake until it reached the equilibrium.

Effect of pH on the Dye Adsorption Property

As mentioned above, the prepared MXH samples were sensitive to the pH value of solutions. The effect of pH on adsorption of MB onto hydrogel sample (MXH-13) was studied, and the results are shown in Fig. 5. In the pH range from 2 to 8, the adsorption amount of MB increased prominently from 3.7 mg/g to 296.8 mg/g, and the dye removal ratio also increased from 11.7% to 99.0%. When the pH was increased to 10, the adsorption amount and the dye removal percentage hardly increased (297.6 mg/g and 99.2%, respectively). A similar trend was seen in some pH sensitive polymers (Paulino *et al*. 2006). This was attributed to the structure of the hydrogel in different pH conditions and also to the interactions between dye molecules and the polymer network. At a lower pH, the shrinkage of hydrogel hindered the MB penetrating into the hydrogel. The MB cations compete with H^+ ions for the adsorption sites in hydrogel, resulting in a very low adsorption. As the pH was increased, the COOH group was converted to COO^- ions, which interacted with MB cations. Besides, the expansion of the hydrogel polymer network was favorable for MB adsorption on the hydrogel. As a result, the adsorption amount of MB and the MB dye removal ratio showed a rising trend. However, the adsorption amount tended to be stable at pH>8 owing to the fixed number of bonding sites of the hydrogel.

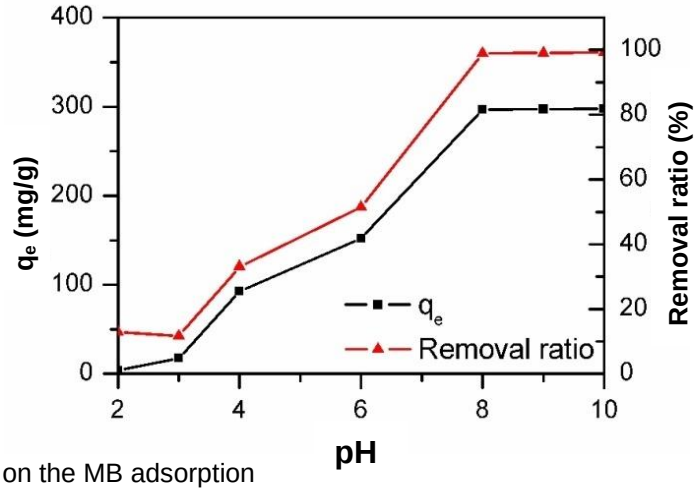

Fig. 5. Effect of pH on the MB adsorption

Effect of Initial MB Concentration and Isotherm Studies

Figure 6 presents the effect of the initial MB concentration on the adsorption property of the xylan-based hydrogel (MXH-13). The amount of MB adsorbed on the porous MXH sample clearly increased from 2490 mg/g to 4690 mg/g as the initial concentration increased from 500 mg/L to 1800 mg/L. This result may be ascribed to the higher concentration of the dye solution inducing a stronger driving force (Sun *et al*. 2015a). However, the MB removal ratio decreased from 99.5% to 53.9% with increasing initial MB concentration. This can be attributed to the limited adsorption sites available on the hydrogel.

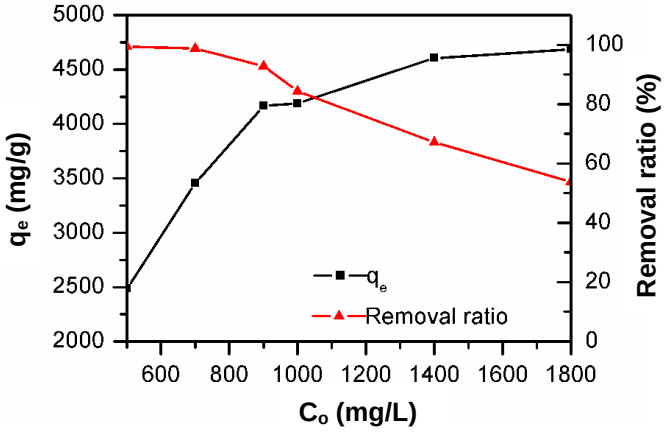

Fig. 6. Effect of initial MB concentration on the adsorption

Two adsorption isotherm models, the Langmuir model and the Freundlich model, were used to investigate the equilibrium adsorption data of MB on the MXH superabsorbent. Langmuir isotherm, presented as Eq. 4, describes a monolayer adsorption on a homogeneous surface (Sun *et al*. 2015b). The Freundlich isotherm is an empirical equation described as Eq. 5 and it is used for heterogeneous multilayer adsorption occurred on solid surfaces (Wang *et al*. 2017).

$$\frac{C_e}{q_e} = \frac{C_e}{q_m} + \frac{1}{q_m b} \quad (4)$$

$$\ln q_e = \frac{1}{n} C_e + \ln K_f \quad (5)$$

In these equations, C_e (mg/L) is the equilibrium MB concentration, q_m (mg/g) is the maximum adsorption capacity, q_e (mg/g) is the amounts of adsorbed MB at equilibrium, b and K_f are the Langmuir constant and the Freundlich constant, and n (L/mg) is a Freundlich parameter, related to the adsorption capacity. Generally, greater n value shows more favorable adsorption performance.

The isothermal parameters from the two models are listed in Table 1. As shown, the coefficient of determination (R^2) of the Langmuir model was 0.999, much larger than that of Freundlich model (0.887). This indicated that the Langmuir isotherm is better than Freundlich isotherm for describing the MB molecular adsorption on the hydrogel by a monolayer adsorption. Based on the Langmuir model, the calculated maximum adsorption capacity of the hydrogel was 4720 mg/g, which was very close to the experimental data of 4690 mg/g. In addition, this number was much larger than that of the reported xylan-containing absorbents (Jing *et al*. 2014; Sun *et al*. 2015b; Qi *et al*. 2017) and

polysaccharides based superabsorbents (Zhu *et al*. 2017; Tang *et al*. 2018), which suggested that the prepared MXH sample exhibited great adsorption performance.

Table 1. Isothermal Parameters of the MXH Adsorbent

$q_{m,exp}$ (mg/g) [a]	Langmuir model			Freundlich model		
	q_m (mg/g)	b (L/mg)	R^2	K_f ($mg^{1-1/n}L^{1/n}g^{-1}$)	n	R^2
4685.7	4717.0	0.13	0.999	2517.5	10	0.887
[a] Experimental data						

Effect of Contact Time and the Adsorption Kinetic Analysis

The time-dependent adsorption of MB on the hydrogel was measured, and the respective adsorption curves are shown in Fig. 7. The amount of MB adsorbed increased rapidly in the first 120 min and reached an essentially static state after that. The MB removal ratio increased from 32.6% to 95.4% at the first stage and then reached 99.0% at 720 min. This suggested that the contact time played an important role in the initial adsorption stage.

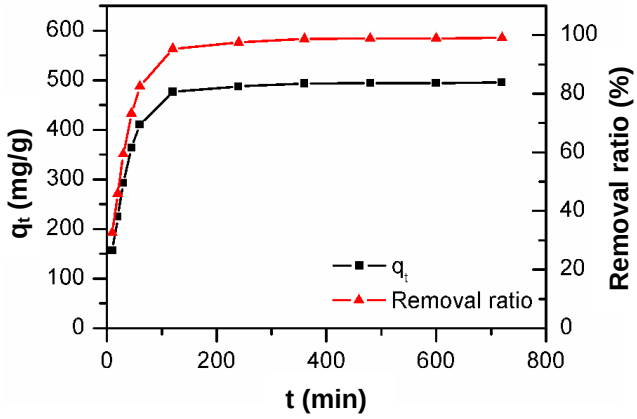

Fig. 7. Effect of contact time on the adsorption

Four kinetic models, the pseudo 1st kinetic model (Eq. 6), the pseudo 2nd kinetic model (Eq. 7) (Li *et al*. 2014), intra-particle diffusion model (Eq. 8) (Lin *et al*. 2018), and Elovich equation (Eq. 9) (Sun *et al*. 2015b), were applied to analyze the adsorption kinetic data for investigating the adsorption process,

$$\lg(q_e - q_t) = \lg q_e - \frac{k_1 t}{2.303} \quad (6)$$

$$\frac{t}{q_t} = \frac{1}{k_2 q_e^2} + \frac{t}{q_e} \quad (7)$$

$$q_t = k_i t^{0.5} + C \quad (8)$$

$$q_t = \frac{1}{b}\ln(ab) + \frac{1}{b}\ln t \quad (9)$$

where q_e and q_t (mg/g) are the amounts of MB adsorbed at equilibrium and at time t, respectively; k_1 (min^{-1}), k_2 ($g \cdot mg^{-1} \cdot min^{-1}$), k_i ($mg \cdot g^{-1} \cdot min^{-1/2}$); and a ($mg \cdot g^{-1} \cdot min^{-1}$) represent the rate constants of the pseudo 1st order, pseudo 2nd order, the intraparticle diffusion, and Elovich equation models, respectively; C (mg/g) is a constant that

characterizes the thickness of the boundary layer; *b* (g/mg) is related to the extent of surface coverage, and the activation energy for the chemisorptions.

The parameters of the four kinetic models are listed in Table 2. As shown in Table 2, the R^2 of the pseudo 2nd model was 0.999, which was higher than that of the other three models, and the calculated q_e predicted in pseudo 2nd model was very close to the measured value. This result indicated that the adsorption of MB on the MXH superabsorbent followed the pseudo 2nd kinetic model. Besides, the intercept C of the fitted curve of the intra-particle diffusion was not 0, which meant that the intra-particle diffusion was not the sole rate-limiting step in the adsorption process.

Table 2. Adsorption Kinetic Parameters of the MXH Adsorbent

Pseudo 1st Order Model			Pseudo 2nd Order Model			Intra-particle Diffusion model			Elovich Equation		
$k_1\times10^{-3}$ (min^{-1})	q_e (mg/g)	R^2	$k_2\times10^{-4}$ ($g\cdot mg^{-1}\cdot min^{-1}$)	q_e (mg/g)	R^2	k_i ($g\cdot g^{-1}\cdot min^{-1/2}$)	C	R^2	*a* (mg/g·min^{-1})	*b* (g/mg)	R^2
9.2	220.8	0.917	1.1	511.0	0.999	11. 8	242.1	0.676	119.1	0.013	0.871
* Experimental data: q_e*(mg/g) = 495.1											

Reusability of the Superabsorbent

The reusability performance of the hydrogel (MXH-13) is summarized in Table 3. In the first two cycles, there were almost no decreases in the removal efficiency. The removal efficiency decreased in the late two cycles because of the decreased adsorption amount with increasing number of cycles. While after 4 adsorption-desorption cycles, the MB removal efficiency of the superabsorbent was maintained above 90%. These results revealed that the xylan-based hydrogel could be regenerated and reused, and have the potential as superabsorbent for MB removal in aqueous solution.

Table 3. Reusability of the Xylan-based Superabsorbent

Recycle times	1	2	3	4
MB (removal efficiency, %)	99.2	98.5	95.8	94.2

CONCLUSIONS

1. A novel porous xylan-based hydrogel was prepared using methacrylated xylan and acrylic acid *via* free radical polymerization reaction. The structure, morphology, and thermal stability of the hydrogel were characterized using FT-IR, SEM, and TGA.
2. The pH played great role with respect to the swelling ratio and MB dye adsorption of the hydrogel. The MXH sample presented excellent MB adsorption performance at pH>8.
3. According to the Langmuir isotherm, the maximum adsorption capacity of the hydrogel reached 4720 mg/g.
4. The MXH can be regenerated and recycled, and the MB removal efficiency was maintained above 90% even after 4 cycles.

ACKNOWLEDGMENTS

The work was financially supported by the Natural Science Foundation of Jiangsu Province (Grant No.: BK20160151) and the Fundamental Research Funds for the Central Non-profit Research Institution of CAF (Grant No.: CAFYBB2019GC001-13).

REFERENCES CITED

Cheng, H. L., Feng, Q. H., Liao, C. A., Liu, Y., Wu, D. B., and Wang, Q. G. (2016). "Removal of methylene blue with hemicelluloses/clay hybrid hydrogels," *Chinese Journal of Polymer Science* 34(6), 709-719. DOI: 10.1007/s10118-016-1788-2

Chen, Q., Yu, H., Wang, L., Abdin, Z., Yang, X., and Wang, J. (2016). "Synthesis and characterization of amylase grafted poly(acrylic acid) and its application in ammonia adsorption," *Carbohydrate Polymers* 153, 429-434. DOI: 10.1016/j.carbpol.2016.07.120

Dai, Y. J., Sun, Q. Y., Wang, W. S., Lu, L., and Liu, M. (2018). "Utilizations of agricultural waste as adsorbent for the removal of contaminants: A review," *Chemosphere* 211, 235-253. DOI: 10.1016/j.chemosphere.2018.06.179

de Azevedo, A. C. N., Vaz, M. G., Gomes, R. F., Pereira, A. G. B., Fajardo, A. R., and Rodrigues, F. H. A. (2017). "Starch/rice husk ash based superabsorbent composite: High methylene blue removal efficiency," *Iranian Polymer Journal* 26(2), 93-105. DOI: 10.1007/s13726-016-0500-2

Deng, A., Chen, J., Li, H., Ren, H., Ren, J., Sun, R., and Zhao, L. (2014). "Photo-degradation of methyl orange by polysaccharides/$LaFe_{0.8}Cu_{0.2}O_3$ composites films," *BioResources* 9(2), 2717-2726. DOI: 10.15376/biores.9.2.2717-2726

Gomes, R. F., de Azevedo, A. C. N., Pereira, A. G. B., Muniz, E. C., Fajardo, A. F., and Rodrigues, F. H. A. (2015). "Fast dye removal from water by starch-based nanocomposites," *Journal of Colloid and Interface Science* 454, 200-209. DOI: 10.1016/j.jcis.2015.02.026

Guilherme, M. R., Reis, A. V., Takahashi, S. H., Rubira, A. F., Feitosa, J. P., and Muniz, E. C. (2005). "Synthesis of a novel superabsorbent hydrogel by copolymerization of acrylamide and cashew gum modified with glycidyl methacrylate," *Carbohydrate Polymers* 61(4), 464-471. DOI: 10.1016/j.carbpol.2005.06.017

Jing, Z., Zhang, G., Sun, X., Shi, X., and Sun, W. (2014). "Preparation and adsorption properties of a novel superabsorbent based on multiwalled carbon nanotubes-xylan composite and poly(methacylic acid) for methylene blue from aqueous solutions," *Polymer Composites* 35(8), 1516-1527. DOI: 10.1002/pc.22805

Katheresan, V., Kansedo, J., and Lau, S. Y. (2018). "Efficiency of various recent wastewater dye removal methods: A review," *Journal of Environmental Chemical Engineering* 6(4), 4676-4697. DOI: 10.1016/j.jece.2018.06.060

Kumari, S., Chauhan, G. S., and Ahn, J. H. (2016). "Novel cellulose nanowhiskers-based polyurethane foam for rapid and persistent removal of methylene blue from its aqueous solutions," *Chemical Engineering Journal* 304, 728-736. DOI: 10.1016/j.cej.2016.07.008

Li, M., and Buschle-Diller, G. (2017). "Pectin-blended anionic polysaccharide films for cationic contaminant sorption from water," *International Journal of Biological Macromolecules* 101, 481-489. DOI: 10.1016/j.ijbiomac.2017.03.091

Li, L., Luo, C., Li, X., Duan, H, and Wang, X. (2014). "Preparation of magnetic ionic liquid/chitosan/graphene oxide composite and application for water treatment," *International Journal of Biological Macromolecules* 66(5), 172-178. DOI: 10.1016/j.ijbiomac.2014.02.031

Li, W., Mu, B. N., and Yang, Y. Q. (2019). "Feasibility of industrial-scale treatment of dye wastewater via bio-adsorption technology," *Bioresource Technology* 277, 157-170. DOI: 10.1016/j.biotech.2019.01.002

Lin, Y., Fang, G. G., Deng, Y. J., Shen. K. Z., Wu, T., and Li, M. (2018). "Highly effective removal of methylene blue using a chemi-mechanical pretreated cellulose-based superabsorbent hydrogel," *BioResources* 13(4), 8709-8722. DOI: 10.15376/biores.13.4.8709-8722

Liu, Z., Xu, D., Zhao, X., Xia, N., and Yang, G. (2018). "Preparation and application of carboxymethylated xylan as a flocculant for ethyl violet dye in aqueous systems," *Journal of Wood Chemistry and Technology* 38(4), 324-337. DOI: 10.1080/02773813.2018.1488874

Mall, I. D., Srivastava, V. C., Agarwal, N. K., and Mishra, I. M. (2005). "Removal of congo red from aqueous solution by bagasse fly ash and activated carbon: kinetic study and equilibrium isotherm analysis," *Chemosphere* 61(4), 492-501. DOI: 10.1016/j.chemosphere.2005.03.065

Melo, B. C., Paulino, F. A. A., Cardoso, V. A., Pereira, A. G. B., Fajardo, A. R., and Rodrigues, F. H. A. (2018). "Cellulose nanowhiskers improve the methylene blue adsorption capacity chitosan-*g*-poly(acrylic acid) hydrogel," *Carbohydrate Polymers* 181, 358-367. DOI: 10.1016/j.carbpol.2017.10.079

Mohammed, N., Grishkewich, N., Berry, R. M., and Tam, K. C. (2015). "Cellulose nanocrystal-alginate hydrogel beads as novel adsorbents for organic dyes in aqueous solutions," *Cellulose* 22(6), 3725-3738. DOI: 10.1007/s10570-015-0747-3

Paulino, A. T., Guilherme, M. R., Mattoso, L. H. C., and Tambourgi, E. B. (2010). "Smart hydrogels based on modified gum Arabic as potential device for magnetic biomaterial," *Macromolecular Chemistry and Physics* 211(11), 1196-1205. DOI: 10.1002/macp.200900657

Paulino, A. T., Guiherme, M. R., Reis, A. V., and Campese, G. M. (2006). "Removal of methylene blue dye from an aqueous media using superabsorbent hydrogel supported on modified polysaccharide," *Journal of Colloid and Interface Science* 301(1), 55-62. DOI: 10.1016/j.jcis.2006.04.036

Peng, X., Ren, J., Zhong, L., Sun, R., Shi, W., and Hu, B. (2012). "Glycidyl methacrylate derivatized xylan-rich hemicelluloses: Synthesis and characterization," *Cellulose* 19(4), 1361-1372. DOI: 10.1007/s10570-012-9718-0

Qi, Y., Yang, M., Xu, W., He, S., and Men, Y. (2017). "Natural polysaccharides-modified graphene oxide for adsorption of organic dyes from aqueous solutions," *Journal of Colloid and Interface Science* 486, 84-96. DOI: 10.1016/j.jcis.2016.09.058

Song, X., Chen, F., and Liu, S. (2016). "A lignin-containing hemicelluloses-based hydrogel and its adsorption behavior," *BioResources* 11(3), 6378-6392. DOI: 10.15376/biores.11.3.6378-6392

Sun, X. F., Gan, Z., Jing, Z. X., Wang, H. H., Wang, D., and Jin, Y. N. (2015a). "Adsorption of methylene blue on hemicelluloses-based stimuli-responsive porous hydrogel," *Journal of Applied Polymer* 132(10), 41606-41615. DOI: 10.1002/app.41606

Sun, X. F., Liu, B. C., Jing, Z. X., and Wang, H. H. (2015b). "Preparation and adsorption

property of xylan/poly(acrylic acid) magnetic nanocomposite hydrogel adsorbent," *Carbohydrate Polymers* 118, 16-23. DOI: 10.1016/j.carbpol.2014.11.013

Tang, Y., He, T., Liu, Y., Zhou, B., Yang, R., and Zhu, L. (2018). "Sorption behavior of methylene blue and rhodamine B mixed dyes onto chitosan graft poly(acrylic acid-*co*-2-acrylamide-2-methyl propane sulfonic acid) hydrogel," *Advances in Polymer Technology* 37(8), 2568-2578. DOI: 10.1002/adv.21932

Tang, Y., Wang, X., and Zhu, L. (2013). "Removal of methyl orange from aqueous solutions with poly(acrylic acid-*co*-acrylamide) superabsorbent resin," *Polymer Bulletin* 70(3), 905-918. DOI: 10.1007/s00289-013-0910-7

Van Dijk-Wolthuis, W. N. E., Franssen, O., Talsma, H., van Steenbergen, M. J., Kettenes-van den Bosch, J. J., and Hennink, W. E. (1995). "Synthesis, characterization, and polymerization of glycidyl methacrylate derivatized dextran," *Macromolecules* 28(18), 6317-6322. DOI: 10.1021/ma00122a044

Van Dijk-Wolthuis, W. N. E., Kettenes-van den Bosch, J. J., van der Kerk-van Hoof, A., and Hennink, W. E. (1997). "Reaction of dextran with glycidyl methacrylate: An unexpected transesterification," *Macromolecules* 30(11), 3411-3413. DOI: 10.1021/ma961764v

Wang, Q., Tian, S., Cun, J., and Ning, P. (2013). "Degradation of methylene blue using a heterogeneous Fenton process catalyzed by ferrocene," *Desalination and Water Treatment* 51(28-30), 5821-5830. DOI: 10.1080/19443994.2012.763047

Wang, N., Jin, R. N., Omer, A. M., and Ouyang, X. K. (2017). "Adsorption of Pb(II) from fish sauce using carboxylated cellulose nanocrystal: Isotherm, kinetics, and thermodynamic studies," *International Journal of Biological Macromolecules*102, 232-240. DOI: 10.1016/j.ijbiomac.2017.03.150

Xu, R., Mao, J., Peng, N., Luo, X. G., and Chang, C. Y. (2018). "Chitin/clay microspheres with hierarchical architecture for highly efficient removal of organic dyes," *Carbohydrate Polymers* 188, 143-150. DOI: 10.1016/j.carbpol.2018.01.073

Yu, S. J., Wang, X. X., Pang, H. W., Zhang, R., and Song, W. C. (2018). "Boron nitride-based materials for the removal of pollutants from aqueous solutions: A review," *Chemical Engineering Journal* 333,343-360. DOI: 10.1016/j.cej.2017.09.163

Zhang, J., Xiao, H., and Zhao, Y. (2014). "Hemicellulose-based absorbent toward dye: Adsorption equilibrium and kinetics studies," *Journal of Environmental Informatics* 24(1), 32-38. DOI: 10.3808/jei.201400270

Zhou, Y., Fu, S., Liu, H., and Yang, S. (2011). "Removal of methylene blue dyes from wastewater using cellulose-based superadsorbent hydrogels," *Polymer Engineering and Science* 51(12), 2417-2424. DOI: 10.1002/pen.22020

Zhu, L., Guan, C., Zhou, B., Zhang, Z., Yang, R., Tang, Y., and Yang, J. (2017). "Adsorption of dye onto sodium alginate graft poly(acrylic acid-*co*-2-acrylamide-2-methyl propane sulfonic acid)/kaolin hydrogel composite," *Polymers and Polymer composites* 25(8), 627-634. DOI: 10.1177/096739111702500808

Article submitted: March 31, 2019; Peer review completed: May 14, 2019; Revised version received: May 21, 2019; Accepted: May 22, 2019; Published: May 29, 2019.
DOI: 10.15376/biores.14.3.5573-5585